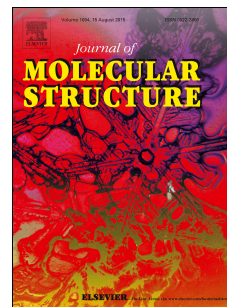


Accepted Manuscript

Synthesis, biological evaluation and *in silico* studies of tetrazole-heterocycle hybrids

Rajendran Sribalan, Govindharasu Banuppriya, Maruthan Kirubavathi, Vediappen Padmini



PII: S0022-2860(18)30941-4

DOI: [10.1016/j.molstruc.2018.07.114](https://doi.org/10.1016/j.molstruc.2018.07.114)

Reference: MOLSTR 25519

To appear in: *Journal of Molecular Structure*

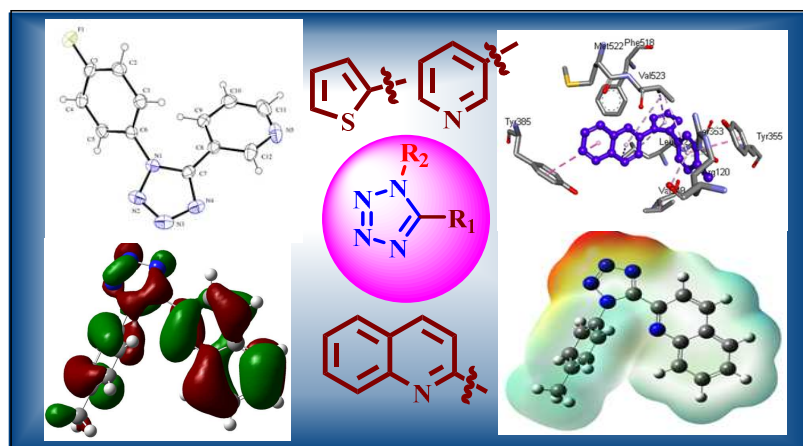
Received Date: 22 February 2018

Revised Date: 30 July 2018

Accepted Date: 31 July 2018

Please cite this article as: R. Sribalan, G. Banuppriya, M. Kirubavathi, V. Padmini, Synthesis, biological evaluation and *in silico* studies of tetrazole-heterocycle hybrids, *Journal of Molecular Structure* (2018), doi: 10.1016/j.molstruc.2018.07.114.

This is a PDF file of an unedited manuscript that has been accepted for publication. As a service to our customers we are providing this early version of the manuscript. The manuscript will undergo copyediting, typesetting, and review of the resulting proof before it is published in its final form. Please note that during the production process errors may be discovered which could affect the content, and all legal disclaimers that apply to the journal pertain.



Synthesis, Biological evaluation and *in silico* studies of Tetrazole-Heterocycle hybrids

Rajendran Sribalan, Govindharasu Banuppriya, Maruthan Kirubavathi, Vediappen Padmini*

Department of Organic Chemistry, School of Chemistry, Madurai Kamaraj University, Madurai-625 021, TamilNadu, India.

*Corresponding author e-mail: padimini_tamilenthi@yahoo.co.in

Abstract

The series of three different chemical entities of tetrazole-heterocycle hybrids such as thiophene, pyridine and quinoline tetrazoles were synthesized and characterized for the purpose to develop a new lead molecules. Biological evaluations such as *in vitro* antimicrobial and anti-inflammatory activities were studied. Further, the *in silico* studies such as Molecular docking (with COX-1, COX-2 and 3TTZ), DFT calculations, the Molecular electrostatic potential (MEP) and ADME were investigated.

Keywords: Hybrid tetrazole, antimicrobial, anti-inflammatory, Molecular docking, Molecular orbitals.

1. Introduction

The studies of the biological importance of a single heterocyclic compounds and their derivatives are interesting area in the field of medicinal chemistry [1]. This due to the fact that 75% of the available drugs in the market are heterocycle based drugs. Also, the introduction of heterocycle on a molecule can change the physiochemical properties such as absorption, distribution, metabolism and excretion [2]. Several heterocyclic compounds have been proved as bioactive compounds [3]. Among various bioactive heterocyclic compounds, the tetrazoles and their derivatives have attracted much attention in drug design [4]. Moreover, these derivatives have several biological activities such as antimicrobial [5], antiviral [6], anti-inflammatory [7], anticancer [8], antidiabetic [9] and antitumor [10]. Losartan, Irbesartan and Valsartan are the

some of the drugs containing 5-aryl tetrazole unit. 1,5-disubstituted tetrazoles based drugs have been used as an antibiotic (Flomoxef, cefazolin sodium and cefonicid) and anticonvulsant drug. Another advantage of tetrazole is a bio-isosteres of carboxylic acids [11]. Based on the literature reports, we have chosen 1,5-disubstituted tetrazole as a bioactive core in our research [12,13]. We expected the combination of another heterocycle on 5th position of tetrazole will contribute to biological applications. So we designed and synthesis of the tetrazole derivatives with various basic heterocycles such as thiophene, pyridine, quinoline and studied for their preliminary biological evaluations such as antimicrobial and anti-inflammatory activities.

Many heterocyclic compounds are biologically potent compound, but active only in *in vitro* level. Most of the compounds are failed in further pharmacological studies (like *in vivo* and other pharmacological studies). So there is a various unresolved problem in drug design. The main drawback of drug designing is that the bioactive compounds (*in vitro* level) are failed in pharmacological studies such as absorption, distribution, metabolism, excretion and toxicity (ADMET). And also some of them are not obeying Lipinski rule of five. On considering the above facts, we carried out molecular docking studies against bacterial DNA Gyrase (3TTZ) and inflammation responsible proteins namely 1PGG (cyclooxygenase-1) and 4COX (cyclooxygenase-2)]. The possible binding orientations are identified with the DFT calculation and Molecular electrostatic potential (MEP), which could explain the binding site of the ligand and also it will be helpful to design new drugs for further improvement. Hence the *in silico* ADMET studies were performed and presented here.

2. Experimental Section

2.1 General consideration

All the chemicals and solvents (laboratory grade) were purchased from sigma Aldrich or Merck. The solvents were used without any purification. Melting points were recorded on sigma melting apparatus SL111140. IR spectrums were recorded in JASCO FT-IR410 using KBr pellet making method. ^1H NMR & ^{13}C NMR spectra were recorded on Bruker 300 MHz and 75 MHz instrument in CDCl_3 with TMS as an internal standard or DMSO-d_6 for proton and carbon spectra. Chemical shift values are mentioned in δ (ppm) and coupling constants are given in Hz. Mass spectra were recorded on AB SCIEX 3000 LC-MS and LCQ Fleet mass spectrometer, Thermo Fisher Instruments Limited, US. Electrospray ionization mass spectrometric method (ESI-MS). The progress of all reactions was monitored by TLC on 2×5 cm pre-coated silica gel 60 F254 plates of a thickness of 0.25 mm (Merck). The single crystal X-ray analysis was recorded in Bruker Kappa APEXII single crystal X-ray diffractometer (Enraf Nonlus CAD4-MV31), SAIF, IIT Madras. The elemental analyses were recorded in vario EL III CHNS element analyzer.

2.2 Chemistry

2.2.1. General procedure for the synthesis of amides (1a-m)

To a DMF solution (3 mL) of carboxylic acid (2.00 mmol), was added at 0°C carbonyl diimidazole (2.2 mmol). The mixture was stirred for 30 minutes at room temperature. To that solution corresponding amine (2.00 mmol) was added. The reaction mixture was stirred for 24 hours at room temperature. The completion of the reaction was monitored by TLC. The reaction mixture was quenched with crushed ice (50 g) and extracted with ethyl acetate (100mL). The organic layer was washed with water (100 mL) and brine solution (100 mL). The organic layer

was separated, dried over anhydrous sodium sulfate and evaporated under reduced pressure. The obtained product was taken to the next step.

2.2.2. General procedure for the synthesis of tetrazole (2a–m)

To an amide (1.01 mmol), phosphorus oxychloride (10.15 mmol) and sodium azide (4.06 mmol) was added. The reaction mixture was stirred for 9 hours at 80 °C under a nitrogen atmosphere and then it was cooled carefully quenched with ice water and neutralized with saturated sodium bicarbonate solution. The product was extracted with ethyl acetate (75 mL), washed with water (2 x 75 mL) and brine solution (75 mL). The organic layer was separated and dried over anhydrous Na₂SO₄ and concentrated under reduced pressure.

2.2.2.1. 1-butyl-5-(thiophen-2-yl)-1H-tetrazole (2a)

Pale Yellowish oil, ¹H NMR (300 MHz, CDCl₃): δ ppm: 7.67 – 7.63 (m, 2H), 7.29-7.23 (m, 1H), 4.60 – 4.52 (m, 2H), 2.04 – 1.91 (m, 2H), 1.50 – 1.40 (m, 2H), 0.98 (t, *J* = 7.3 Hz, 3H). ¹³C NMR (75 MHz, CDCl₃): δ ppm: 149.39, 130.25, 129.91, 128.40, 124.24, 48.12, 31.41, 19.66, 13.42. ESI-LC/MS calculated *m/z* 208.2 found 209.1 (*M*⁺+1). IR (KBr) *ν*_{max}: 3103, 2960, 1572, 1475, 715. Anal.Calcd for: C₉H₁₂N₄S: C, 51.90; H, 5.81; N, 26.90 %. Found: C, 51.93; H, 5.79; N, 26.89 %.

2.2.2.2. 1-(4-fluorophenyl)-5-(thiophen-2-yl)-1H-tetrazole (2b)

Colourless solid, Mp: 143-145 °C, ¹H NMR (300 MHz, CDCl₃): δ ppm: 7.57 – 7.46 (m, 3H), 7.37 – 7.28 (m, 3H), 7.20-7.06 (m, 1H). ¹³C NMR (75 MHz, CDCl₃): δ ppm: 165.62, 162.26, 150.02, 130.89, 130.73, 130.03, 128.71, 128.59, 128.21, 124.00, 117.50, 117.19. ESI-LC/MS calculated *m/z* 246.0, found 247.1 (*M*⁺+1). IR (KBr) *ν*_{max}: 3076, 1568, 1269, 1155, 1097. Anal.Calcd for: C₁₁H₇FN₄S: C, 53.65; H, 2.87; N, 22.75 %. Found: C, 53.68; H, 2.88; N, 22.72 %.

2.2.2.3. 1-phenyl-5-(thiophen-2-yl)-1H-tetrazole (2c)

Reddish Brown solid, Mp: 87-88 °C, ¹H NMR (300 MHz, CDCl₃): δ ppm: 7.64 – 7.59 (m, 3H), 7.52 – 7.47 (m, 3H), 7.27 – 7.24 (m, 1H), 7.06 - 7.03 (m, 1H). ¹³C NMR (75 MHz, CDCl₃): δ ppm: 149.82, 134.01, 131.27, 130.71, 130.55, 130.10, 128.10, 126.35, 124.15. ESI-LC/MS calculated m/z 228.0, found 229.2 (M⁺+1). IR (KBr) ν_{max}: 3078, 1551, 1267, 1123, 1095, 1020. Anal.Calcd for: C₁₁H₈N₄S: C, 57.88; H, 3.53; N, 24.54 %. Found: C, 57.89; H, 3.56; N, 24.51 %.

2.2.2.4. 1-(methylsulfonyl)-4-(5-(thiophen-2-yl)-1H-tetrazol-1-yl)piperidine (2d)

Colourless solid, Mp: 163-165 °C, ¹H NMR (300 MHz, CDCl₃): δ ppm: 7.69 (dd, *J* = 5.1, 1.1 Hz, 1H), 7.64 (dd, *J* = 3.7, 1.1 Hz, 1H), 7.32 – 7.27 (m, 1H), 4.82 – 4.73 (m, 1H), 3.99 – 3.87 (m, 2H), 3.19 – 3.07 (m, 2H), 2.89 (s, 3H), 2.50 – 2.38 (m, 2H), 2.33 – 2.24 (m, 2H). ¹³C NMR (75 MHz, CDCl₃): δ ppm: 148.69, 130.25, 129.82, 128.18, 123.18, 54.78, 43.95, 35.24, 30.97. ESI-LC/MS calculated m/z 313.1 found 314.2 (M⁺+1). IR (KBr) ν_{max}: 2937, 1479, 1249, 1168, 1085, 1058, 949. Anal.Calcd for: C₁₁H₁₅N₅O₂S₂: C, 42.16; H, 4.82; N, 22.35 %. Found: C, 42.15; H, 4.81; N, 22.35 %.

2.2.2.5. 3-(1-butyl-1H-tetrazol-5-yl)pyridine (2e)

Pale yellowish oil, ¹H NMR (300 MHz, CDCl₃): δ ppm: 8.94 – 8.85 (m, 2H), 8.10 - 8.07 (m, 1H), 7.56 (dd, *J* = 7.8, 4.9 Hz, 1H), 4.46 (t, *J* = 7.4 Hz, 2H), 2.05 – 1.90 (m, 2H), 1.38 - 1.33 (m, 2H), 0.93 (t, *J* = 7.3 Hz, 3H). ¹³C NMR (75 MHz, CDCl₃): δ ppm: 152.27, 152.00, 148.90, 136.51, 124.51, 48.19, 31.81, 19.67, 13.39. ESI-LC/MS calculated m/z 203.1, found 204.2 (M⁺+1). IR (KBr) ν_{max}: 2962, 2933, 1570, 1464, 707. Anal.Calcd for: C₁₀H₁₃N₅: C, 59.10; H, 6.45; N, 34.46 %. Found: C, 59.13; H, 6.46; N, 34.47 %

2.2.2.6. 2-(1-cyclohexyl-1H-tetrazol-5-yl)pyridine (2f)

White solid, Mp: 125-128 °C, ^1H NMR (300 MHz, CDCl_3): δ ppm: 8.94 – 8.78 (m, 2H), 8.07 – 7.99 (m, 1H), 7.58 – 7.53 (m, 1H), 4.37 – 4.26 (m, 1H), 2.26 – 2.02 (m, 5H), 2.02 – 1.93 (m, 2H), 1.47 – 1.30 (m, 3H). ^{13}C NMR (75 MHz, CDCl_3): δ ppm: 152.15, 151.28, 149.00, 136.64, 124.08, 121.20, 58.67, 33.34, 25.21, 24.72. ESI-LC/MS calculated m/z 229.2 found 230.2 ($\text{M}^+ + 1$). IR (KBr) ν_{max} : 3078, 2933, 1568, 1462, 705. Anal. Calcd for: $\text{C}_{12}\text{H}_{15}\text{N}_5$: C, 62.86; H, 6.59; N, 30.54 %. Found: C, 62.88; H, 6.58; N, 30.56 %.

2.2.2.7. 3-(1-(4-fluorophenyl)-1H-tetrazol-5-yl)pyridine (2g)

Colourless solid, Mp: 120-121 °C, ^1H NMR (300 MHz, CDCl_3): δ ppm: 8.76 – 8.74 (m, 2H), 8.00 – 7.93 (m, 1H), 7.48 – 7.38 (m, 3H), 7.27 (m, 2H). ^{13}C NMR (75 MHz, CDCl_3): δ ppm: 165.32, 161.96, 152.32, 151.65, 149.26, 136.28, 130.19, 127.61, 127.49, 123.85, 120.17, 117.69, 117.39. ESI-LC/MS calculated m/z 241.2 found 242.2 ($\text{M}^+ + 1$). IR (KBr) ν_{max} : 3076, 1504, 1226, 1134, 1097, 1024, 993. Anal. Calcd for: $\text{C}_{12}\text{H}_8\text{FN}_5$: C, 59.75; H, 3.34; N, 29.03 %. Found: C, 59.74; H, 3.36; N, 29.04 %.

2.2.2.8. 3-(1-benzyl-1H-tetrazol-5-yl)pyridine (2h)

Colourless solid, Mp: 98-100 °C, ^1H NMR (300 MHz, CDCl_3): δ ppm: 8.82 – 8.72 (m, 1H), 7.99 – 7.90 (m, 1H), 7.52 – 7.44 (m, 1H), 7.36-7.25 (m, 3H), 7.17 – 7.13 (m, 2H), 5.67 (s, 2H). ^{13}C NMR (75 MHz, CDCl_3): δ ppm: 152.35, 152.28, 149.04, 136.40, 133.43, 129.36, 129.03, 127.11, 123.86, 120.50, 51.70. ESI-LC/MS calculated m/z 237.2 found 238.1 ($\text{M}^+ + 1$). IR (KBr) ν_{max} : 3051, 2926, 1568, 1454, 704. Anal. Calcd for: $\text{C}_{13}\text{H}_{11}\text{N}_5$: C, 65.81; H, 4.67; N, 29.52 %. Found: C, 65.80; H, 4.69; N, 29.54 %.

2.2.2.9. 2-(1-butyl-1H-tetrazol-5-yl)quinoline (2i)

Pale yellowish oil, ^1H NMR (300 MHz, CDCl_3): δ ppm: 8.47 – 8.32 (m, 2H), 8.13 (d, $J = 8.5$ Hz, 1H), 7.92 (d, $J = 8.1$ Hz, 1H), 7.86 – 7.79 (m, 1H), 7.70 – 7.64 (m, 1H), 5.21 – 5.10 (m, 2H),

2.12 – 1.99 (m, 2H), 1.50 - 1.45 (m, 2H), 1.01 (t, $J = 7.4$ Hz, 3H). ^{13}C NMR (75 MHz, CDCl_3): δ ppm: 151.58, 147.28, 144.69, 137.43, 130.39, 129.54, 128.19, 128.05, 127.79, 120.88, 118.68, 49.66, 31.83, 19.63, 13.52. ESI-LC/MS calculated m/z 253.3, found 254.4($\text{M}^+ + 1$). IR (KBr) ν_{max} : 3061, 2960, 1599, 1498, 767. Anal. Calcd for: $\text{C}_{14}\text{H}_{15}\text{N}_5$: C, 66.38; H, 5.97; N, 27.65 %. Found: C, 66.39; H, 5.96; N, 27.64 %.

2.2.2.10. 2-(1-cyclohexyl-1H-tetrazol-5-yl)quinoline (2j)

White solid, Mp: 82-85 °C, ^1H NMR (300 MHz, CDCl_3): δ ppm: 8.44 – 8.34 (m, 2H), 8.13 (d, $J = 8.5$ Hz, 1H), 7.92 (d, $J = 7.4$ Hz, 1H), 7.85 – 7.78 (m, 1H), 7.71 – 7.63 (m, 1H), 5.82 – 5.75 (m, 1H), 2.33 – 2.93 (m, 2H), 2.17 – 2.08 (m, 4H), 1.99 – 1.81 (m, 2H), 1.58 – 1.40 (m, 4H). ^{13}C NMR (75 MHz, CDCl_3): δ ppm: 151.40, 147.51, 145.30, 137.57, 130.49, 129.92, 128.33, 127.97, 121.49, 60.12, 32.96, 25.71, 25.27. ESI-LC/MS calculated m/z 279.3 found 280.2 ($\text{M}^+ + 1$). IR (KBr) ν_{max} : 2929, 1502, 1462, 763. Anal. Calcd for: $\text{C}_{16}\text{H}_{17}\text{N}_5$: C, 68.79; H, 6.13; N, 25.07 %. Found: C, 68.76; H, 6.11; N, 25.08 %.

2.2.2.11. 2-(1-(1-(methylsulfonyl)piperidin-4-yl)-1H-tetrazol-5-yl)quinoline (2k)

Colourless solid, Mp: 208-210 °C, ^1H NMR (300 MHz, CDCl_3): δ ppm: 8.47 – 8.38 (m, 2H), 8.09 (d, $J = 8.4$ Hz, 1H), 7.95 (d, $J = 8.1$ Hz, 1H), 7.88 – 7.81 (m, 1H), 7.72 – 7.67 (m, 1H), 6.00 – 5.96 (m, 1H), 4.08 – 3.99 (m, 2H), 3.23 – 3.11 (m, 2H), 2.93 (s, 3H), 2.52 – 2.44 (m, 4H). ^{13}C NMR (75 MHz, CDCl_3): δ ppm: 151.67, 147.52, 145.03, 137.95, 130.78, 129.73, 128.64, 128.49, 128.14, 121.52, 56.86, 44.84, 36.45, 31.54. ESI-LC/MS calculated m/z 357.1 found 358.2 ($\text{M}^+ + 1$). IR (KBr) ν_{max} : 3009, 1496, 1101, 1249, 1157, 1018, 966. Anal. Calcd for: $\text{C}_{16}\text{H}_{18}\text{N}_6\text{O}_3\text{S}$: C, 51.33; H, 4.85; N, 22.45 %. Found: C, 51.35; H, 4.86; N, 22.47%.

2.2.2.12. 2-(1-(p-tolyl)-1H-tetrazol-5-yl)quinoline (2l)

Colourless solid, Mp: 126-128 °C, ^1H NMR (300 MHz, CDCl_3): δ ppm: 8.34 – 8.24 (m, 2H), 7.87 (d, $J = 8.1$ Hz, 1H), 7.75 - 7.71 (m, 2H), 7.65 – 7.58 (m, 1H), 7.44 (d, $J = 8.3$ Hz, 2H), 7.32 (d, $J = 8.0$ Hz, 2H), 2.49 (s, 3H). ^{13}C NMR (75 MHz, CDCl_3): δ ppm: 152.81, 147.57, 144.28, 140.35, 137.40, 133.36, 130.39, 130.05, 129.56, 128.40, 127.80, 126.16, 121.37, 21.44. ESI-LC/MS calculated m/z 287.1, found 288.2 ($\text{M}^+ + 1$). IR (KBr) ν_{max} ; 3069, 1555, 1264, 1146, 1094, 1009. Anal. Calcd for: $\text{C}_{17}\text{H}_{13}\text{N}_5$: C, 71.06; H, 4.56; N, 24.37 %. Found: C, 71.05; H, 4.60; N, 24.39 %.

2.2.2.13. 2-(1-(naphthalen-1-yl)-1H-tetrazol-5-yl)quinoline (2m)

Colourless solid, Mp: 110-113 °C, ^1H NMR (300 MHz, CDCl_3): δ ppm: 8.39 – 8.24 (m, 2H), 8.12 - 7.99 (m, 1H), 8.01 (d, $J = 8.3$ Hz, 1H), 7.76 (dd, $J = 6.0, 3.6$ Hz, 1H), 7.66 – 7.59 (m, 2H), 7.57 – 7.51 (m, 1H), 7.51 – 7.45 (m, 2H), 7.44 – 7.37 (m, 1H), 7.21 (d, $J = 8.5$ Hz, 1H), 7.05 (dd, $J = 6.1, 3.6$ Hz, 1H). ^{13}C NMR (75 MHz, CDCl_3): δ ppm: 154.11, 147.21, 143.41, 137.27, 133.95, 132.75, 130.87, 130.13, 129.91, 129.82, 128.31, 128.25, 128.13, 127.79, 127.55, 126.93, 125.39, 124.88, 122.17, 120.70. ESI-LC/MS calculated m/z 323.1, found 324.2 ($\text{M}^+ + 1$). IR (KBr) ν_{max} ; 3059, 1595, 1253, 1145, 1109, 1039. Anal. Calcd for: $\text{C}_{20}\text{H}_{13}\text{N}_5$: C, 74.29; H, 4.05; N, 21.66 %. Found: C, 74.30; H, 4.07; N, 21.66 %.

2.3. Biology and *in silico* studies

2.3.1 Antibacterial activity

The bacterial strains used for the examinations were *K. pneumoniae* (ATCC 13883), *P. aeruginosa* (ATCC 10145), *S. aureus* (ATCC 11632), *S. pyogenes* (ATCC 12358) and *C. albicans* (ATCC 66027) obtained from either American type culture collection or purchased from Himedia, Mumbai. The experiments were repeated twice. The experimental technique used is as followed by Sribalan *et al* [14].

2.3.2. Anti-inflammatory activity

The synthesized compounds were tested for anti-inflammatory activity (bovine serum albumin denaturation technique). The experimental technique used is as followed by Sribalan *et al* [15].

2.3.3. Molecular docking study

Molecular docking of compounds into the bacterial enzyme, COX-1 and COX-2 enzymes was carried out using the Auto-Dock software (version 4.2)[16,17]. Accelrys discovery studio client 4.1 was used for the visualizing protein-ligand complex. Three dimensional structures of synthesized derivatives were optimized using the Gaussian 09W software (for the ligand). The crystal structure of the bacterial enzyme, COX-1 and COX-2 (3TTZ.pdb, 1PGG.pdb and 4COX.pdb) were downloaded from Protein Data bank. All bound water and ligand were eliminated from the protein and polar hydrogen was added. Moreover all docking, a grid box size of 60x60x60 points in X, Y and Z direction. A grid spacing of 0.375 Å and ten runs were generated by using Lamarckian genetic algorithm searches.

2.3.4. Computational calculations

All the computational calculations including representation of Highest occupied molecular orbital (HOMO) and Lowest unoccupied molecular orbital (LUMO) in the checkpoint files was performed with the Gaussian 09W program using density functional theory [18]. The chemical structure of the compound was optimized with B3LYP/6.311 ++ G (d,p) basis set. The Gauss view software package was used to visualize the computed structures including HOMO, LUMO and Molecular electrostatic potential (MEP) representations.

2.3.5. ADME calculations

The pharmacological properties like molar volume (MV), topological polar surface area (TPSA) and Lipinski rule of five were calculated using Molinspiration online tool [19]. The Absorption (% ABS) was calculated by the formula $\% \text{ABS} = 109 - (0.345 \times \text{TPSA})$ [20] and the aqueous solubility was calculated using online admetSar tools [21].

3. Results and Discussion

3.1. Chemistry

The designed heterocyclic tetrazoles were synthesized from their corresponding amide precursors which are represented in Scheme 1. The amides can be prepared from their corresponding acids and amines with the use of coupling agent like carbonyl diimidazole [22]. The reaction of amides with phosphorus oxychloride and sodium azide yielded tetrazoles [23]. The synthesized compounds were characterized by ^1H NMR, ^{13}C NMR, Mass and IR spectroscopies. The disappearance of amide peak in proton NMR clearly indicates the conversion of the amide. Similarly, the disappearance of amide carbonyl peak in the region 160 ppm and the appearance of tetrazolyl carbon in the region of 155 ppm clearly indicate the tetrazoles formation. The ESI-Mass spectrum also attributed the tetrazoles formation. The mass spectrum clearly showed the molecular ion peaks for the tetrazoles either in positive mode or in negative mode. Similarly, the IR spectrum also gave the additional evidence for the disappearance of the carbonyl stretching frequency ($1600\text{-}1650\text{ cm}^{-1}$) and appearance new absorbance which is due to the formation of tetrazoles.

For example, in the characterization of **2a**, the disappearance of amide peak at 6.08 ppm in ^1H NMR and disappearance of amide carbonyl peak at 162.1 ppm in ^{13}C NMR indicates the complete conversion of the amide. The appearance of a new peak at 149.3 ppm in ^{13}C NMR

indicates the formation of tetrazolyl carbon. The multiplet at 7.66-7.64 ppm for 2 protons and multiplet at 7.29-7.23 ppm for one proton indicates the presence of thiophene ring. The multiplet around 4.62-4.50 ppm for 2 protons indicates the presence of CH₂ unit which was attached to tetrazole ring nitrogen. The remaining multiplets around 1.99–1.90 for 2 protons, 1.45–1.42 for 2 protons and 0.98 ppm for 3 protons indicates the presence of *n*-butyl unit. In the ¹³C NMR, the peaks at 130.25, 129.91, 128.40 and 124.24 ppm indicate the presence of thiophene ring. The peaks at 48.12, 31.41, 19.66 and 13.42 ppm indicate the presence of *n*-butyl unit. The ESI-Mass clearly showed the peak at 209.1 in a positive mode which also confirms the product formation. In the FT-IR spectrum, the band around 3103 cm⁻¹ indicates the presence of aromatic C-H units (thiophene C-H units). The band around 1572 cm⁻¹ indicates the presence of C=N unit. Similarly, the band around 1475 cm⁻¹ indicates the presence of N=N unit. In addition, the compound 2g was confirmed by single crystal X-ray analysis (Fig. 1) (CCDC No: 996387). This list of synthesized compounds is represented in Fig. 2.

3.2. Biology

3.2.1. Antimicrobial activity

A series of heterocyclic tetrazoles were screened for antimicrobial activity against the bacterias such as *Klebsiella pneumoniae* (ATCC 13883), *Pseudomonas aeruginosa* (ATCC 27853), *Staphylococcus aureus* (ATCC 25923), *Streptococcus pyogenes* (ATCC 12358) and fungal pathogen *Candida albicans* (ATCC 66027). Except the compound 2f, all the compounds showed the activity against *Klebsiella pneumoniae*. The compound 2e has the pyridyl ring and *n*-butyl unit showed better inhibition than the standard drug (amikacin) and the compound 2k bearing quinoline and piperidyl sulfonamide unit showed comparable inhibition to the standard. The compounds 2b, 2c, 2d, 2g, 2h, 2j, 2l and 2m showed the moderate activity against the

Klebsiella pneumoniae. The compound **2k** showed the low activity against *Pseudomonas aeruginosa* and the compound **2d**, **2h** and **2j** exhibited the moderate activity against *Pseudomonas aeruginosa*. The compound **2b** bearing thiophene and *p*-fluoro phenyl unit showed potent activity against *Staphylococcus aureus*. The compounds **2c**, **2e**, **2i**, **2l** and **2m** showed low to moderate activity against the *Staphylococcus aureus*. Similarly, the compound **2k**, bearing the quinoline and piperidyl sulphonamide unit showed good inhibition against *Streptococcus pyogenes*. The compounds **2d**, **2h**, **2i**, **2j** and **2l** showed moderate activity against *Streptococcus pyogenes*. Some of the compounds showed the antifungal activity. Among those compounds, **2b** having the thiophene and phenyl ring showed good activity against *Candida albicans*. The compounds **2a**, **2c** and **2g** showed moderate activity against a fungal pathogen. Overall, the synthesized compounds showed better to good zone of inhibition than parent thiophene, quinoline, pyridine and tetrazole. The zone of inhibitions of the compounds, standard and parent were listed in Table 1.

3.2.2. Anti-inflammatory activity

All the synthesized compounds were studied for their *in vitro* anti-inflammatory activity by using inhibition of albumin denaturation technique with minor modification. The activities of the compounds were checked with four different concentrations of 50 µg/mL, 100 µg/mL, 200 µg/mL and 400 µg/mL respectively. Diclofenac sodium was used as the standard drug. All the compounds showed moderate to good anti-inflammatory activity. The compound **2b** and the compound **2i** showed a good percentage of inhibition, which is almost equal to the standard diclofenac sodium. Other than these, all the compounds showed moderate anti-inflammatory activity. Overall, the synthesized compounds showed good to moderate anti-inflammatory

activity than parent thiophene, quinoline, pyridine and tetrazole. The various concentrations of compounds, standard, and parent's percentage inhibitions were listed in Table 2.

3.2.3. ADME prediction

All the synthesized heterocyclic hybrids have been screened for *in silico* ADME properties by using online tool Molinspiration and ADMETSar. The molecular weights of compounds are in the range of 208-358 g/mol. The log P value (partition coefficient in octanol-water) is 1.01-4.18. The numbers of hydrogen bond acceptor in the ligands are 4-8. A number of hydrogen bond donors are zero. The Molar volumes of the synthesized compounds are in the range of 186-283. Hence all the compounds are obeying the Lipinski rule of five. Also, the other parameters have been checked such as TPSA (topological polar surface area), Q log p and number of rotatable bonds. All the values calculated for the synthesized compounds are comparable with the 95% ideal drugs in the market [24]. The percentage absorption is calculated from topological polar surface area [%ABS = 109 – (0.345 x TPSA)]. Usually, the compounds having more than 80% absorption can be considered as a good drug. Among these compound except 2d (72%) and 2k (67%), all the other compounds have good absorption (>80%). Some of the compounds showed around 93 % absorption. From all the above prediction, we theoretically suggest that all the synthesized compounds have very good ADME properties. The ADME properties for the synthesized compounds are represented in Table 3.

3.2.4. Molecular Docking studies

3.2.4.1. DNA gyrase inhibition (3TTZ)

DNA gyrase inhibition is one of the mechanisms for preventing the bacterial replication process which induces bacterial death [25]. Some nitrogen based heterocyclic drugs are used as a DNA gyrase inhibitor (Nalidixic acid, ciprofloxacin). On the basis of this idea, the enzyme 3TTZ

(DNA gyrase enzyme) was chosen for docking. All the synthesized compounds were docked with the DNA gyrase enzyme 3TTZ to identify the possible protein-ligand interaction. Generally, the ligands are binding with protein *via* various interactions such as pi-alkyl interaction, pi-donor hydrogen bond interaction and conventional hydrogen bond interaction.

Nitrogen in the synthesized compounds can form hydrogen bond with the amino acid of the enzyme. Similarly, the thiophene based derivatives also showed the conventional hydrogen bond interactions with the amino acid. But the nitrogen present in either pyridine derivative or quinoline derivative did not show any conventional hydrogen bond interactions. Most of the compounds showed hydrogen bond with the amino acid GLY85 of the enzyme 3TTZ. But the compound **2d** showed the hydrogen bond with the amino acid GLU58 and the compound **2f** showed the hydrogen bond with the amino acid SER129. In the compound **2f**, the tetrazole nitrogen form the hydrogen bond with hydroxyl hydrogen (N---HO) of SER129. In the compounds **2c**, **2e**, **2h** and **2i**, the tetrazole nitrogen interacted by the hydrogen bond with peptide nitrogen of GLY85 (N---HN). The entire group of synthesized compounds exhibited very good bind energies and inhibition constants. The binding energies are in the range of -5.97 to -9.06 kcal/mol and inhibition constant values in the range of 51.96 to 0.22 μ M. Among the various compounds, the compound **2m** quinoline tetrazoles containing naphthalene ring showed highest binding energy and inhibition constant. Overall, the quinoline tetrazoles derivative showed very good binding interactions with DNA gyrase enzyme than the thiophene and pyridyl tetrazoles derivatives. The model protein-ligand complex (**2l** with 3TTZ) is represented in Fig. 3. The Docking energy, inhibition constant and hydrogen bonding of ligand-protein complexes were represented in Table 4.

3.2.4.1. Cyclooxygenase inhibition

The synthesized compounds exhibited *in vitro* anti-inflammatory activity. Cyclooxygenase is one of the enzymes responsible for producing prostaglandin. The cyclooxygenase enzyme inhibition will provide pain relief and cure inflammation [26]. On the basis of this, the protein 1PGG and 4COX were chosen for docking. All the synthesized compounds were docked with COX-1(1PGG) and COX-2(4COX) enzyme. Similar to the DNA gyrase, the docking against cyclooxygenase showed several interactions with COX-1 (1PGG) enzyme. Among the 13 synthesized hybrids, the compound **2b** and **2c** containing *n*-butyl and *p*-fluoro phenyl substituents showed hydrogen bonding with SER530 of 1PGG. Similarly, the compounds **2e**, **2f** and **2g** containing *n*-butyl, cyclohexyl and *p*-fluoro phenyl substituents showed hydrogen bond with SER530 of 1PGG. The compound **2m** quinoline tetrazoles containing naphthalene ring showed hydrogen bond with TYR385. The hydrogen bonds are Pi-donor hydrogen bonds which were formed between aromatic ring of the synthesized compounds and the hydrogen of the amino acid (SER530 or TYR385). All the compounds showed very good binding energies (-7.11 to -11.35 kcal/mol) and inhibition constants (6.11 to 0.004 μ M). Within this series, the quinoline based tetrazoles **2j**, **2k**, **2l** and **2m** showed highest binding energy which is -11.35, -10.25, -10.76 and -10.87 kcal/mol and their inhibition constants are 0.004, 0.032, 0.012 and 0.010 μ M respectively. In the overall docking of the COX-1 enzyme with the synthesized compounds, quinoline based tetrazoles derivative showed better docking results than thiophene and pyridyl tetrazoles. Similarly, the synthesized compounds were docked with a COX-2 enzyme (4COX). Most of the compounds showed hydrogen bond interaction with amino acid of the COX-2 enzyme as similar to COX-1. The thiophene and pyridine based tetrazoles (**2a-h**) showed the hydrogen bond with SER530. The compound **2a** thiophene tetrazole containing *n*-butyl substituents exhibited the conventional hydrogen bond interaction between

tetrazole nitrogen and hydroxyl group of SER530 (N---HO). The compound **2h** containing benzyl substituent showed both conventional and pi-donor hydrogen bond interactions with SER530 (N---HO, Tet---HO). In the compounds **2b**, **2c**, **2f** and **2i**, the tetrazole rings have shown the pi-donor hydrogen bond interaction with hydroxyl of SER530 (Tet---HO). In the case of compound **2a** and **2f**, two hydrogen bond interactions were formed with two amino acids of TYR385 and SER530. The compound **2k** containing piperidine sulphonamide unit showed hydrogen bond with ARG120. The entire list of compounds showed very good binding energies (-6.85 to -10.41 kcal/mol) and inhibition constants (9.47 to 0.023 μ M). Among these derivatives, the compounds **2j**, **2k**, **2l** and **2m** quinoline tetrazoles showed the highest binding energies (-9.37, -10.41, -9.48 and -10.16 kcal/mol) and their inhibition constants were 0.135, 0.023, 0.112 and 0.356 μ M respectively. Overall, quinoline based tetrazoles derivative showed better docking results than thiophene and pyridyl tetrazoles. The model protein-ligand complexes (**2l** with 1PGG and **2l** with 4COX) are represented in Fig. 3 & 4. The binding energy, inhibition constant and hydrogen bonding of COX-1 and COX-2 with amino acids were represented in Table 5 & 6.

3.5. Computational Studies

3.5.1. Frontier molecular orbitals

The highest occupied molecular orbital and lowest unoccupied molecular orbital can be used to predict the most reactive position of the molecule in pi-electron systems. In an organic molecule, the electrons are not assigned to individual covalent bond, which is moving under the whole molecule by the influence of nuclei of the molecule. So the electron density of the molecule has not same in all the region of the molecule. The electron cloud plays a major role in the intermolecular interaction. The protein-ligand docking method depends on various intermolecular interactions such as pi-donor hydrogen bond interaction, pi-alkyl interaction, pi-

sigma interaction and pi-anion interaction. In all compounds, the electron density is more in tetrazole and heterocyclic rings. In some cases (**2c**, **2g**, **2h**, **2l** and **2m**) the additional aromatic side chains also have more electron density in either HOMO or LUMO. So these regions should be responsible for interactions with the protein. The same results were obtained in molecular docking studies, where the interactions were found between the aromatic rings (tetrazole, heterocycle and phenyl ring) and amino acids. Especially the tetrazolyl nitrogen makes the conventional hydrogen bond and pi-donor hydrogen bond with particular amino acids (GLY 85, GLU 58, SER129, SER530, TYR385, TRP387 and ARG120).

Similarly, the thiophene sulphur makes the conventional hydrogen bonding with an amino acid (GLY85, GLU 58, SER 530, TYR 385 and TRP 387). The aliphatic side chains do not have more electron cloud. So there is less interaction with the protein. Comparatively, quinoline tetrazoles have more electron density than the thiophene and pyridine tetrazoles. Probably the quinoline tetrazole **2i**, **2j**, **2k**, **2l** and **2m** have the more interaction with proteins than the others. Among the quinoline tetrazoles, the compounds having the aromatic side chains **2l** and **2m** has better interaction than the others heterocyclic hybrids.

HOMO-LUMO band gap ΔE plays an important role in the chemical stability of the molecule. The band gap values of the synthesized compounds (**2a-m**) are in the range of 4.07 to 5.69 eV. The band gap values clearly indicate the heterocyclic tetrazoles are chemically stable. Similarly, the chemical potential and the global hardness are higher. The chemical potential and hardness of the compounds are in the range of -4.31 to -4.90 eV and 2.03 to 2.84 eV respectively. Also, the global softness of the synthesized compound is 0.17 to 0.24 eV⁻¹. From the results, we suggest the heterocyclic tetrazoles are hard material and chemically stable compound. Comparatively, within this series the stability order is pyridine tetrazoles>thiophene

tetrazole>quinoline tetrazole. The electrophilicity index is measured from chemical hardness and chemical potential of the molecule.

The Electrophilicity is the possible descriptor of biological activity [27] which is the capacity to accept the electrons from the environment. So, higher the electrophilicity index higher will be the binding interaction with the environmental molecule. The electrophilicity index of the synthesized compounds (**2a-m**) is in the range of 3.75 to 5.28. Comparatively the quinoline tetrazole has the more electrophilicity index value than thiophene and pyridine tetrazole derivative. The molecular docking studies also exhibited the similar results, the quinoline tetrazoles having more interaction with the proteins. The global molecular reactive descriptors such as HOMO, LUMO, band gap, chemical potential, global hardness, global softness and electrophilicity index of the heterocycle tetrazole hybrids are represented in Table 7 and coherent with the commercially available drug (paracetamol)[28]. From the DFT results, we suggest that the tetrazole heterocycle hybrids could be better molecules. The Frontier molecular orbital of compound **2l** is represented in Fig. 6.

The above DFT parameters were calculated from the given equations.

$$\text{Band gap} \quad \Delta E = E_{\text{LUMO}} - E_{\text{HOMO}}$$

$$\text{Chemical potential} \quad \mu = (E_{\text{HOMO}} + E_{\text{LUMO}})/2$$

$$\text{Global hardness} \quad \eta = (E_{\text{LUMO}} - E_{\text{HOMO}})/2$$

$$\text{Global softness} \quad \zeta = 1/2\eta$$

$$\text{Electrophilicity index } \omega = \mu^2/2\eta$$

3.5.2. Molecular Electrostatic potential

Molecular electrostatic potential (MEP) displays the charge distribution of molecule in surfaces which can be helpful to find the electrophilic and nucleophilic site of the molecule. And also this is the well suited method for analyzing the process of binding interaction and hydrogen bonding interaction of biomolecules with a ligand which will be helpful to the biological activity of the molecule [29]. The electrophilic site is visually represented in red colour which indicates the negative region of the molecule. The nucleophilic site is blue in colour which indicates the positive region of the molecule. The negative region of the molecule is more important because which is ready to make the hydrogen bonding with protein. Here, all the **13** compounds were studied for molecular electrostatic potential. The MEP clearly showed the negative region is localized over tetrazolyl nitrogen which is probably responsible for hydrogen bonding. The molecular docking studies also proved, the tetrazole ring showed more hydrogen bond with enzymes. The surface nitrogen N2, N3 and N4 of tetrazoles are making the conventional hydrogen bonding with amino acids. In the pyridine tetrazoles (**2e**, **2f**, **2g** and **2h**), the pyridyl nitrogen showed little negative charge which is not involving in hydrogen bonding with the protein (results from molecular docking). The quinoline nitrogen (**2i**, **2j**, **2k**, **2l** and **2m**) has not shown any negative charge and there is no hydrogen bonding with the enzymes (results from molecular docking). The aromatic ring surfaces are the nucleophilic site. Especially the quinoline ring surface clearly showed blue colour which is positive charge region. This may be responsible for the other interactions with the enzyme. Overall the quinoline tetrazoles have both negative and positive charged surface which make this series of molecules to have more interactions with the amino acids of the enzyme. The Molecular electrostatic potential mapping of compound **2l** is represented in Fig. 7.

Conclusions

The tetrazole-heterocycle hybrids exhibited excellent binding with enzymes in both bacterial and inflammatory studies. In the molecules, the tetrazoles are the responsible unit which makes more interaction with the enzyme. The *in silico* pharmacological results for the hybrids were very good which is comparable to the regular drugs. The DFT parameters and MEP clearly explains the tetrazole unit and aromatic regions are more responsible units in biological interaction. Within the series, the quinoline tetrazole exhibited very good results than pyridyl and thiophene tetrazole hybrid. So the tetrazole-heterocycle hybrids may be the lead molecule in further studies. Further the current research is focused to study the experimental binding of the enzyme with heterocyclic tetrazoles.

Acknowledgments

The authors are grateful to UGC and DST, New Delhi for financial support and DST-IRHPA program for providing high resolution NMR facility.

Figures and captions:

Scheme 1. Synthesis of tetrazoles-heterocycle hybrid.

Fig 1. ORTEP diagram of compound **2g**.

Fig .2. List of synthesized compounds (**2a-m**).

Fig. 3. Interaction of compound **2l** with 3TTZ.

Fig. 4. Interaction of compound **2l** with 1PGG.

Fig. 5. Interaction of **2l** with 4COX.

Fig. 6. The HOMO and LUMO of Compound **2l**.

Fig. 7. Molecular electrostatic potential mapping of compound **2l**.

Tables and captions:

Table 1. Antimicrobial activity of heterocyclic tetrazoles **2a-m** (Zone of inhibition in mm).

Table 2. Anti-inflammatory activity of heterocyclic tetrazoles **2a-m** (% inhibition).

Table 3. *In silico* physicochemical pharmacokinetic parameters important for good oral bioavailability of synthesized compounds (**2a-m**).

Table 4: Molecular docking interaction of synthesized compounds (**2a-m**) against DNA gyrase.

Table 5: Molecular docking interaction of synthesized compounds (**2a-m**) against 1PGG.

Table 6. Molecular docking interaction of synthesized compounds (**2a-m**) against 4COX.

Table 7: DFT calculations of synthesized compound (**2a-m**).

Reference and notes:

1. R. Dua, S. Shrivastava, S.K. Sonwane, S.K. Srivasta, Pharmacological significance of synthetic heterocycles scaffold: A review, *Adv. Biol. Res.* 5 (2011) 120-144.
2. A. Dennis, *Metabolism, Pharmacokinetics and Toxicity of Functional Groups: Impact of Chemical Building Blocks on ADMET* (2010) DOI: 10.1039/9781849731102-00328.
3. M. S. Saini, A. Kumar, J. Dwivedi, R. Singh, A review: Biological significances of heterocyclic compounds, *Int. J. Pharm. Res.* 4 (2013) 66-77.
4. V. A. Ostrovskii, R. E. Trifonov, E. A. Popova, Medicinal chemistry of tetrazoles, *Russ. Chem. Bull.* 61 (2012) 768-780.
5. M. J. Genin, D. A. Allwine, D. J. Anderson, M. R. Barbachyn, D. E. Emmert, S. A. Garmon et al., Substituent effects on the antibacterial activity of nitrogen-carbon linked(Azolyphenyl)oxazolidinones with expanded activity against the fastidious gram-negative organisms haemophilus influenzae and moraxella catarrhalis, *J. Med. Chem.* 43. (2000) 953-970.

6. M. S. Poonian, E. F. Nowoswiat, J. F. Blount, M. J. Kramer, Synthesis of tetrazole ribonucleosides and their evaluation as antiviral agents. 2. 5-amino-a-(β -ribofuranosyl)-1H-tetrazole and 5-amino-2-(β -D-ribofuranosyl)-2H-tetrazole, *J. Med. Chem.* 19 (1976) 1017-1020.
7. J. R. Maxwell, D. A. Wasdahl, A. C Wolfson, V. I. Stenberg, Synthesis of 5-aryl-2H-tetrazole-2-acetic acids, and [(4-Phenyl-5-aryl-4H-1,2,4-triazol-3-yl)thio]acetic acids as possible superoxide scavengers and antiinflammatory agents, *J. Med. Chem.* 27 (1984) 1565-1570.
8. C. N. S. S. P. Kumar, D. K. Parida, A. Santhoshi, A. K. Kota, B. Sridhar, V. J. Rao, Synthesis and biological evaluation of tetrazole containing compounds are possible anticancer agents, *Med. Chem. Comm.* 2 (2011) 486-492.
9. R. M. Oballa, L. Belair, W. C. Black, K. Bleasby, C. C. Chan, C. Desroches, X. Du, R. Gordon, J. Guay, S. Guiral, M. J. Hafey, E. Hamelin, Z. Huang, B. Kennedy, N. Lachance, F. Landry, C. S. Li, J. Mancini, D. Normandin, A. Poci, D. A. Powell, Y. K. Ramtohol, K. Skorey, D. Sorensen, W. Sturkenboom, A. Styhler, D. M. Waddleton, H. Wang, S. Wong, L. Xu, L. Zhang, Development of a Liver-Targeted Stearoyl-CoA Desaturase(SCD) Inhibitor (MK-8245) to Establish a Therapeutic Window for the Treatment of Diabetes and Dyslipidemia, *J. Med. Chem.* 54 (2011) 5082-5096.
10. K. M. Penov-Gasi, A. M. Okliesa, E. T. Petri, A. S. Celic, E. A. Diurendic, O. R. Ilic, J. J. Csanadi, G. Batta, A. R. Nikolic, D. S. Jakimov, M. N. Sakac. Selective antitumour activity and ER α Molecular docking studies of newly synthesized D-homo fused steroidal tetrazoles, *Med. Chem. Comm.* 4 (2013) 317-323.

11. F. H. Allen, C. R. Groom, J. W. Liebeschuetz, D. A. Bardwell, T. S. Olsson and P. A. Wood, The hydrogen bond environments of 1H-tetrazole and tetrazolate rings: The structural basis for tetrazole-carboxylic acid bioisosterism. *J. Chem. inf. modell.* 52 (2012) 857-866.
12. R. Romagnoli, P. G. Baraldi, M. K. Salvador, D. Preti, M. A. Tabrizi, A. Brancale, X-H. Fu, J. Li, S. Zhang, E. Hamel, R. Bortolozzi, G. Basso, G. Viola, Synthesis and Evaluation of 1,5-Disubstituted Tetrazoles and rigid analogues of combretastatin A-4 with potent antiproliferative and antitumor activity. *J. Med. Chem.* 55 (2012) 476-488.
13. A. Kamal, A. Viswanath, M. J. Ramaiah, J. N. S. R. C. Murty, F. Sultana, G. Ramakrishna, J. R. Tamboli, S. N. C. V. I. Pushpavalli, D. Pal, C. Kishor, A. Addlagatta, M. P. Bhadra, Synthesis of tetrazole-isooxazoline hybrids as a new class of tubulin polymerization inhibitors. *Med. Chem. Commun.* 3 (2012) 1386-1392.
14. R. Sribalan, V. Padmini, A. Lavanya, K. Ponnuvel, Evaluation of antimicrobial activity of glycinate and carbonate derivatives of cholesterol: Synthesis and characterization, *Saudi Pharm. J.* 24 (2016) 658-668.
15. R. Sribalan, M. Kirubavathi, G. Banuppriya, V. Padmini, synthesis and biological evaluation of new symmetric curcumin derivatives, *Bioorg. Med. Chem. Lett.* 25 (2015) 4282-4286.
16. S. M. D. Rizvi, S. Shakil, M. Haneef, A simple click by click protocol to perform docking: autodock 4.2 made easy for non-bioinformaticians, *EXCLI J.* 12 (2013) 831-857.
17. G. Banuppriya, R. Sribalan, V. Padmini, V. Shanmugaiah, Biological evaluation and molecular docking studies of new curcuminoid derivatives: synthesis and characterization, *Bioorg. Med. Chem. Lett.* 26 (2016) 1655-1659.
18. M. J. Frisch, G. W. Trucks, H. B. Schlegel, G. E. Scuseria, M. A. Robb, J. R. Cheeseman, J. A. Montgomery, Jr., T. Vreven, K. N. Kudin, J. C. Burant, J. M. Millam, S. S. Iyengar, J.

- Tomasi, V. Barone, B. Mennucci, M. Cossi, G. Scalmani, N. Rega, G. A. Petersson, H. Nakatsuji, M. Hada, M. Ehara, K. Toyota, R. Fukuda, J. Hasegawa, M. Ishida, T. Nakajima, Y. Honda, O. Kitao, H. Nakai, M. Klene, X. Li, J. E. Knox, H. P. Hratchian, J. B. Cross, V. Bakken, C. Adamo, J. Jaramillo, R. Gomperts, R. E. Stratmann, O. Yazyev, A. J. Austin, R. Cammi, C. Pomelli, J. W. Ochterski, P. Y. Ayala, K. Morokuma, A. Voth, P. Salvador, J. J. Dannenberg, V. G. Zakrzewski, S. Dapprich, A. D. Daniels, M. C. Strain, O. Farkas, D. K. Malick, A. D. Rabuck, K. Raghavachari, J. B. Foresman, J. V. Ortiz, Q. Cui, A. G. Baboul, S. Clifford, J. Cioslowski, S. B. B. tefanov, G. Liu, A. Liashenko, P. Piskorz, I. Komaromi, R. L. Martin, D. J. Fox, T. Keith, M. A. AllLaham, C. Y. Peng, A. Nanayakkara, M. Challacombe, P. M. W. Gill, B. Johnson, W. Chen, M. W. Wong, C. Gonzalez, J. A. Pople, Gaussian 03, Revision C.02, Gaussian, Inc., Wallingford, CT, 2004.
19. Molinspiration Chemoinformatics, Brastislava, Slovak Republic, Available from: <http://www.molinspiration.com/cgi-bin/properties>, (2015).
20. Y. Zhao, M. H. Abraham, J. Lee, A. Hersey, C. N. Luscombe, G. Beck, B. Sherborne, B. I. Cooper, Rate-limited steps of human oral absorption and QSAR studies, *Pharm. Res.* 19 (2002) 1446-1457.
21. F. Cheng, W. Li, Y. Zhou, J. Shen, Z. Wu, G. Liu, P. W. Lee, Y. Tang, admetSAR: A Comprehensive Source and Free Tool for Assessment of Chemical ADMET Properties, *J. Chem. Inf. Model.* 52 (2012) 3099-3105.
22. B. R. Paul, G. W. Anderson, N,N'-Carbonyldiimidazole, a New Peptide Forming Reagent, *J. Am. Chem. Soc.* 82 (1960) 4596-4600.
23. R. Sribalan, A. Lavanya, M. Kirubavathi, V. Padmini, *J. Saudi Chem. Soc.* 22 (2018) 198-207.

24. D. Choudhary, G. K. Gupta, S. L. Khokra, Nisha, Structure based designing and ADME-T studies of betenolide derivatives as potential agents against receptor ICAM-a: A drug target for cerebral malaria, *J. Comp. Sci.* 10 (2015) 156-165.
25. B. A. Sherer, K. Hull, O. Green, G. Basarab, S. Hauck, P. Hill, J. T. Loch, 3rd, G. Mullen, S. Bist, J. Bryant, A. Boriack-Sjodin, J. Read, N. DeGrace, M. Uria-Nickelsen, R. N. Illingworth, A. E. Eakin, Pyrraolamide DNA gyrase inhibitors: optimization of antibacterial activity and efficacy, *Bioorg. Med. Chem. Lett.* 21 (2011) 7416-7420.
26. D. A. Willoughby, A. R. Moore, P. R. Colville-Nash. COX-1, COX-2, and COX-3 and the future treatment of chronic inflammatory disease, *Lancet*, 335 (2000) 646-648.
27. R. Parthasarathi, V. Subramanian, D. R. Roy, P. K. Chattaraj, Electrophilicity index as a possible descriptor of biological activity, *Bioorg. Med. Chem.* 12 (2004) 5533-5543.
28. R. Anitha, M. Gunasekaran, S. S. Kumar, S. Athimoolam, B. Sridhar, Single crystal XRD, vibrational and quantum chemical calculation of pharmaceutical drug paracetamol: A new synthesis form, *Spectrochim. acta, Part A, Mol. biomol. spectrosc.* 150 (2015) 488-498.
29. A. Chidangil, M. K. Shukla, P. C. Mishra, A molecular electrostatic potential mapping study of some fluoroquinolone anti-bacterial agents, *J. Mol. Model.* 4 (1998) 250-258.

Table: 1

Entry	<i>K.Pneumoniae</i>	<i>P.aeruginosa</i>	<i>S. aureus</i>	<i>S.pyogenes</i>	<i>C. albicans</i>
2a	13.2±0.4	-	-	-	11.2±0.3
2b	10.2±0.4	-	15.0±0.1	-	16.1±0.3
2c	10.2±0.2	-	4.1±0.2	-	8.9±0.2
2d	14.2±0.2	10.2±0.3	-	8.0±0.3	-
2e	17.2±0.2	-	7.2±0.3	-	-
2f	-	-	-	-	-
2g	10.1±0.1	-	-	-	8.2±0.1
2h	7.8±0.5	10.2±0.1	-	12.0±0.1	-
2i	10.4±0.3	-	7.1±0.2	8.0±0.2	-
2j	12.2±0.2	12.0±0.3	-	12.2±0.3	-
2k	15.1±0.1	3.9±0.2	-	15.9±0.2	-
2l	10.1±0.3	-	4.6±0.3	8.2±0.3	-
2m	12.1±0.1	-	4.2±0.4	-	-
Thiophene	5.3±0.2	-	-	4.2±0.2	-
Quinoline	6.7±0.2	-	5.2±0.2	5.6±0.2	-
Pyridine	5.8±0.1	4.2±0.2	-	-	4.2±0.2
Tetrazole	8.0±0.3	5.2±0.2	4.6±0.3	10.1±0.2	7.0±0.3
S1					21.2
S2	17.2	17.0	18.2	18.1	

Control – Dimethylsulfoxide: Standard – S1:Ketoconazole for fungi, S2:Amikacin for bacteria.

Table :2

Entry	50µg/mL	100µg/mL	200µg/mL	400µg/mL
2a	11.15±0.80	21.13±0.67	45.77±0.21	53.61±0.45
2b	17.60±0.41	41.93±0.43	63.68±0.23	74.44±1.02
2c	12.41±0.52	28.71±0.31	45.77±0.21	60.21±0.34
2d	11.49±0.34	20.62±0.51	48.32±0.44	57.11±0.65
2e	11.30±0.81	20.21±0.31	47.62±0.65	58.61±0.12
2f	12.60±0.21	25.96±0.44	49.67±1.05	60.21±0.33
2g	12.01±0.32	22.23±0.21	49.83±0.34	58.04±0.23
2h	12.66±0.11	28.71±0.23	47.26±0.78	55.87±0.12
2i	16.30±1.51	37.93±0.87	59.87±0.65	73.31±0.54
2j	13.05±0.45	27.69±0.34	50.64±0.13	61.21±0.54
2l	12.63±0.41	25.96±0.23	49.83±0.76	55.87±0.12
2k	11.06±0.56	21.02±1.20	40.39±0.21	49.83±0.12
2m	12.35±0.67	25.96±0.45	48.14±0.11	53.89±0.65
Thiophene	7.01±0.32	15.98±0.23	33.55±0.45	50.98±1.0
Quinoline	11.01±0.44	22.48±0.33	41.27±0.54	53.12±0.67
Pyridine	6.98±0.54	14.49±0.45	31.92±0.65	48.90±0.98
Tetrazole	10.02±0.32	18.62±0.87	39.25±0.65	52.57±0.45
S3	14.00	20.42	63.61	79.03

Standard-S3: diclofenac sodium

Table: 3

Compound	Abs %	TPS A (A ²)	MV	n-ROT B	MW	mi log P	n-ON acceptors	n-OH/NH donars	QPlogs	Lipinski violations
Ideal Range in 95% of drugs	-	<140	-	<15	<500	<5	<10	<5	-6.5-0.5	<1
2a	93.9	43.61	186.03	4	208.2	2.66	4	0	-1.53	0
2b	93.9	43.61	195.40	2	246.27	2.66	4	0	-2.78	0
2c	93.9	43.61	190.47	4	228.28	2.49	4	0	-1.64	0
2d	72.0	80.99	253.03	3	313.41	1.01	7	0	-2.17	0
2e	80.5	56.50	191.16	4	203.35	1.80	5	0	-1.53	0
2f	80.5	56.50	214.19	2	229.29	2.27	5	0	-1.98	0
2g	80.5	56.50	200.53	2	241.23	1.80	5	0	-3.40	0
2h	80.5	56.50	212.40	3	237.27	1.96	5	0	-1.78	0
2i	80.5	56.50	235.15	4	253.31	2.97	5	0	-2.78	0
2j	80.5	56.50	258.18	2	279.35	3.44	5	0	-2.50	0
2k	67.6	93.88	302.15	3	358.43	1.33	8	0	-3.18	0
2l	80.5	56.50	256.15	2	287.33	3.26	5	0	-2.75	0
2m	80.5	56.50	283.59	2	323.36	4.18	5	0	-2.88	0

Table :4

S. No	Compound Name	Binding energy(kcal/mol)	3TTZ		
			Inhibition constant (μ M)	No. of H-bonding	H-bonded residue
1	2a	-5.97	41.72	1	GLY85
2	2b	-6.39	20.85	1	GLY85
3	2c	-6.42	19.78	1	GLY85
4	2d	-6.86	9.32	1	GLU58
5	2e	-5.84	51.96	1	GLY85
6	2f	-6.54	16.14	1	SER129
7	2g	-6.13	32.22	1	GLY85
8	2h	-6.96	7.94	1	GLY85
9	2i	-7.17	5.58	1	GLY85
10	2j	-8.44	0.62	1	GLY85
11	2k	-8.51	0.58	1	GLY85
12	2l	-8.02	1.32	1	GLY85
13	2m	-9.06	0.22	1	GLY85

Table : 5

S. No	Compound Name	Binding energy (kcal/mol)	1PGG		
			Inhibition constant (μ M)	No. of H-bonding	H-bonded residue
1	2a	-7.11	6.11	-	-
2	2b	-8.37	0.726	1	SER530
3	2c	-8.35	0.763	1	SER530
4	2d	-9.12	0.205	-	-
5	2e	-7.24	4.9	1	SER530
6	2f	-8.81	0.35	1	SER530
7	2g	-8.29	0.842	1	SER530
8	2h	-8.42	0.673	-	-
9	2i	-8.69	0.427	-	-
10	2j	-11.35	0.0047	-	-
11	2k	-10.21	0.032	-	-
12	2l	-10.76	0.012	-	-
13	2m	-10.87	0.010	1	TYR385

Table :6

S. No	Compound Name	4COX			
		Binding energy (kcal/mol)	Inhibition constant (μ M)	No. of H-bonding	H- bonded residue
1	2a	-6.97	7.76	2	TYR385,S ER530
2	2b	-7.71	2.25	1	SER530
3	2c	-7.98	1.42	1	SER530
4	2d	-8.52	0.569	1	TRP387
5	2e	-6.85	9.47	1	SER530
6	2f	-8.37	0.734	2	TYR385,S ER530
7	2g	-7.66	2.44	1	SER530
8	2h	-8.32	0.793	1	SER530
9	2i	-8.21	0.964	1	SER530
10	2j	-9.37	0.135	0	-
11	2k	-10.41	0.023	1	ARG120
12	2l	-9.48	0.112	0	-
13	2m	-10.16	0.356	0	-

Table :7

S. No	Compound name	HOMO	LUMO	Band gap(ΔE)	Chemical potential	Global hardness	Global softness	Electrophilicity index
1.	2a	-6.7948	-1.8368	4.958	-4.315	2.4790	0.2016	3.7568
2.	2b	-6.8846	-2.0599	4.824	-4.472	2.4123	0.2072	4.1456
3.	2c	-6.7839	-1.9619	4.821	-4.372	2.4109	0.2073	3.9657
4.	2d	-7.0506	-2.0164	5.034	-4.533	2.5171	0.1986	4.0826
5.	2e	-7.5567	-1.8585	5.698	-4.707	2.8490	0.1754	3.8893
6.	2f	-7.4860	-1.8422	5.643	-4.664	2.8218	0.1771	3.8545
7.	2g	-7.4969	-2.1524	5.344	-4.824	2.6722	0.1871	4.3554
8.	2h	-7.3935	-1.9429	5.450	-4.668	2.7252	0.1834	3.9981
9.	2i	-6.9662	-2.3919	4.574	-4.679	2.2871	0.2187	4.7862
10.	2j	-6.9635	-2.4028	4.560	-4.683	2.2803	0.2192	4.8089
11.	2k	-7.1758	-2.6286	4.547	-4.902	2.2735	0.2199	5.2850
12.	2l	-6.8846	-2.3892	4.495	-4.636	2.2477	0.2224	4.7828
13.	2m	-6.4655	-2.3946	4.070	-4.430	2.0354	0.2456	4.8210

Scheme 1.

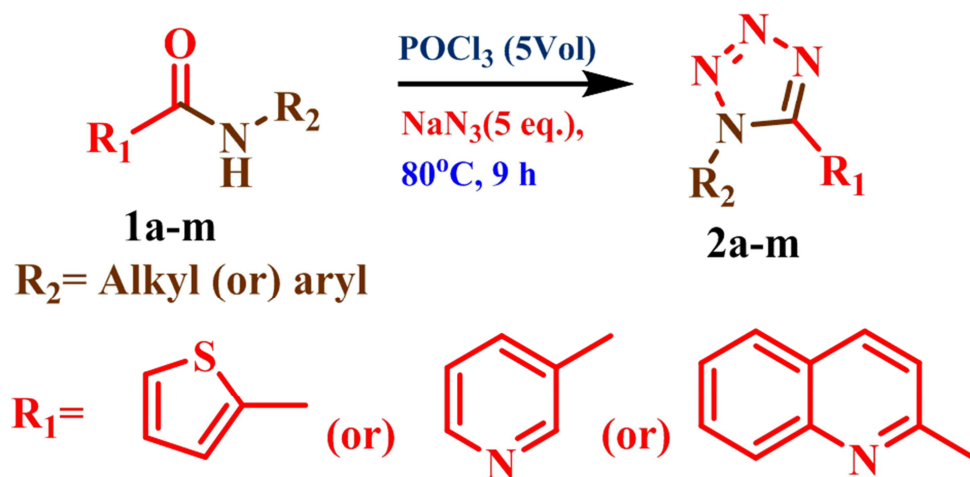


Fig 1.

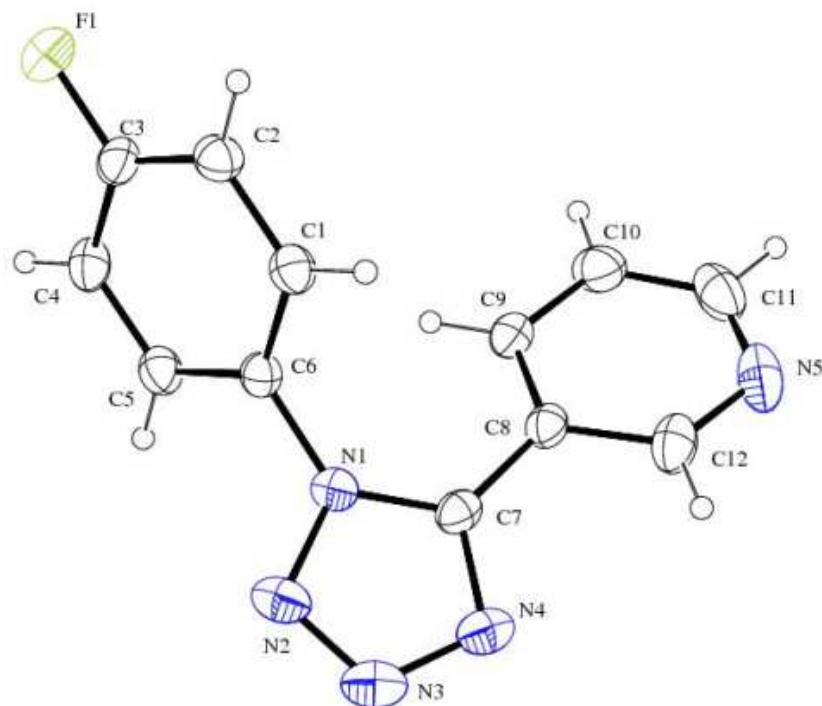


Fig 2.

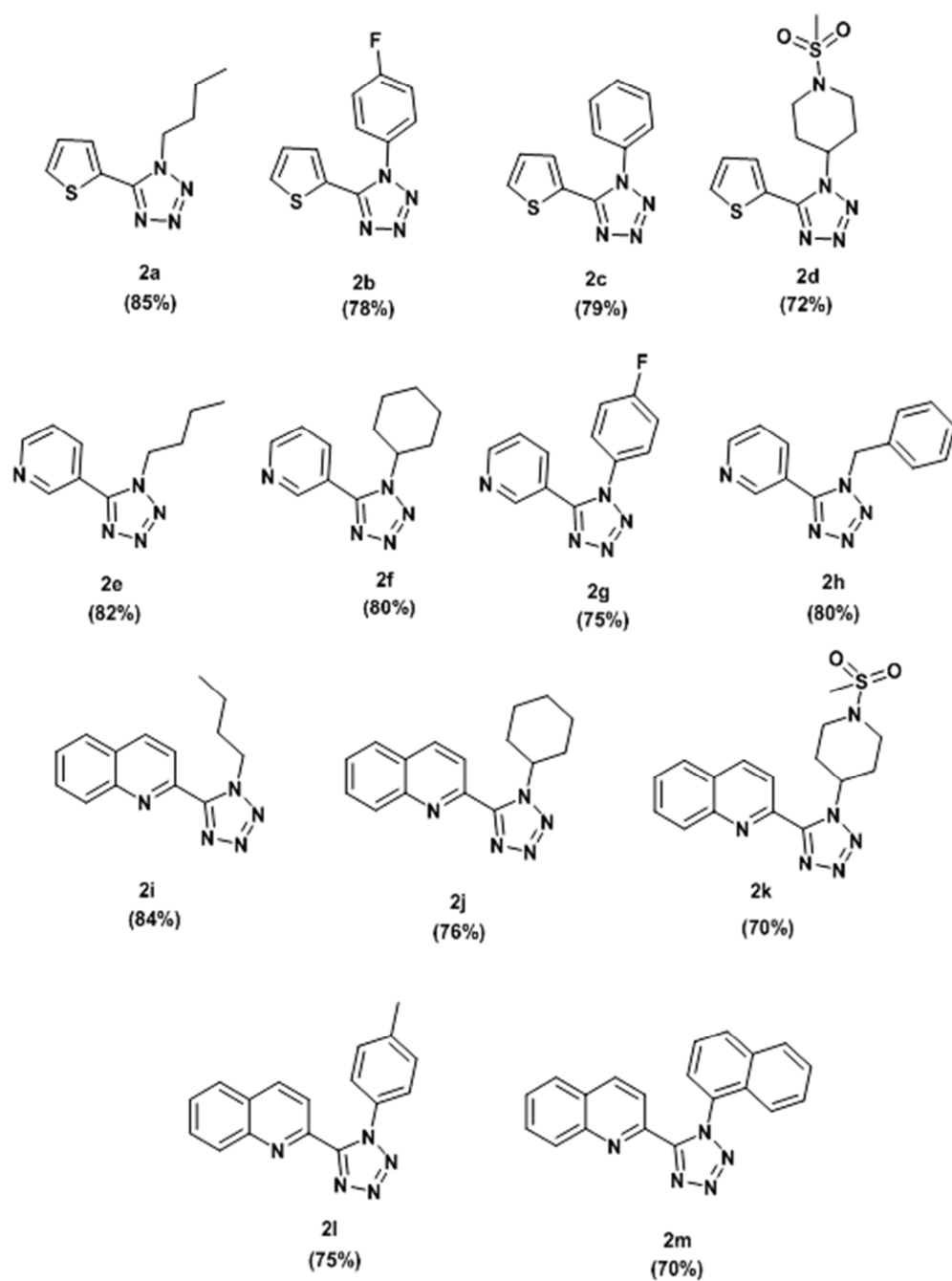


Fig. 3.

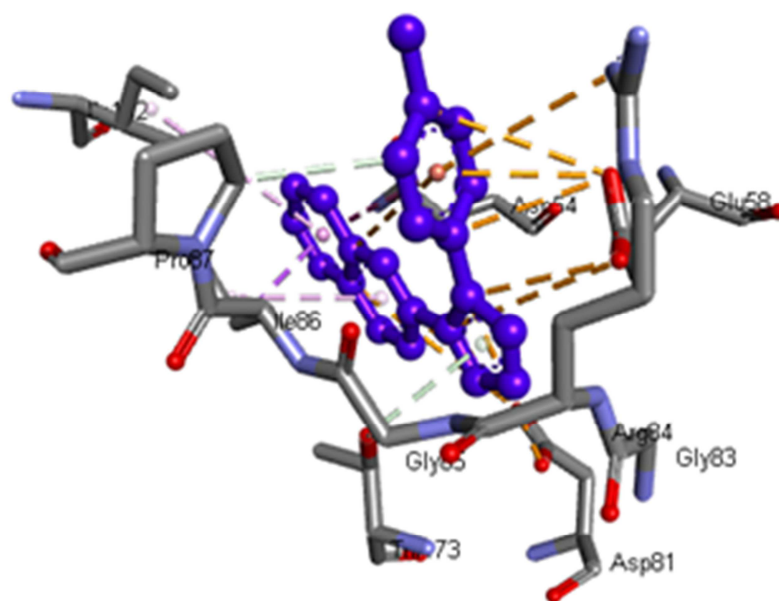


Fig. 4.

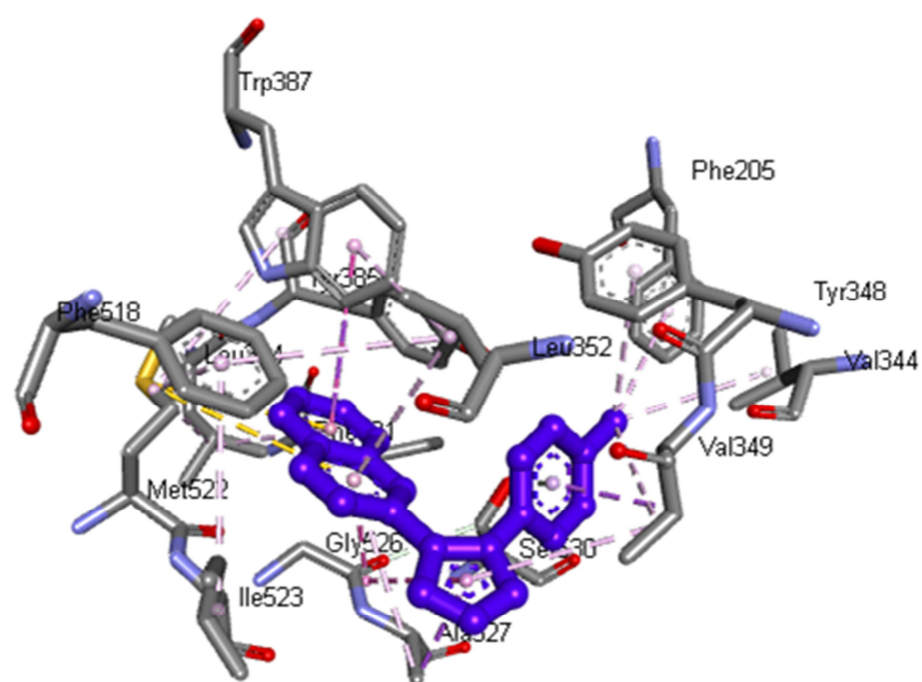


Fig. 5.

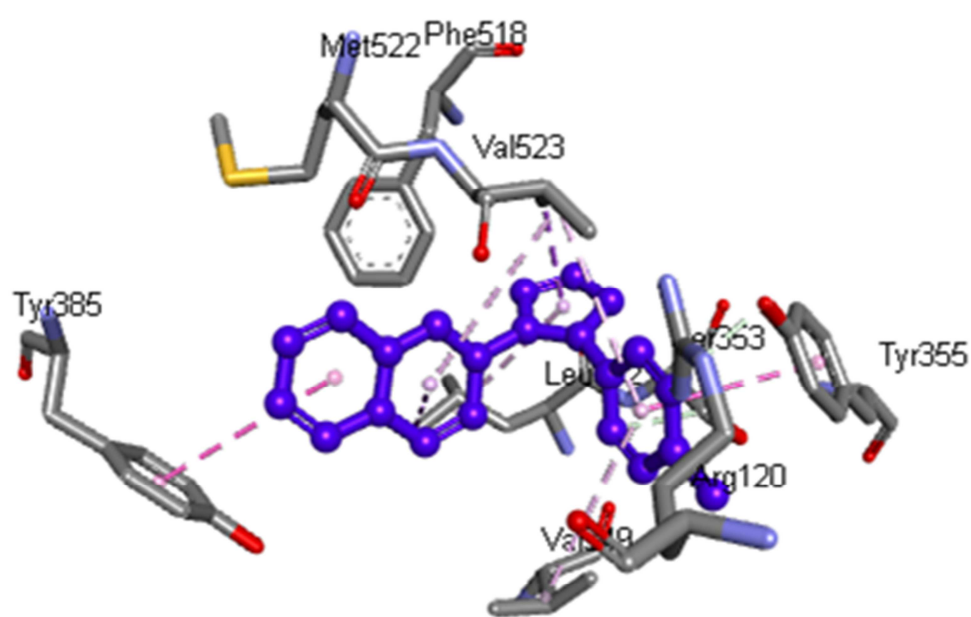


Fig. 6.

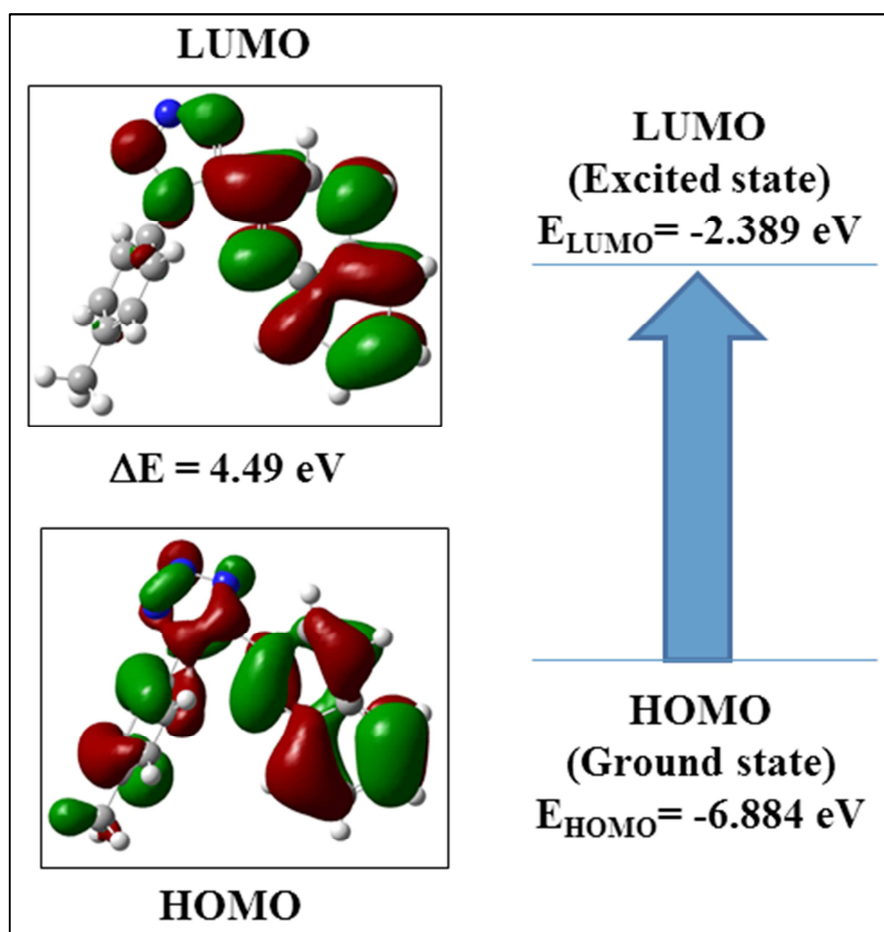
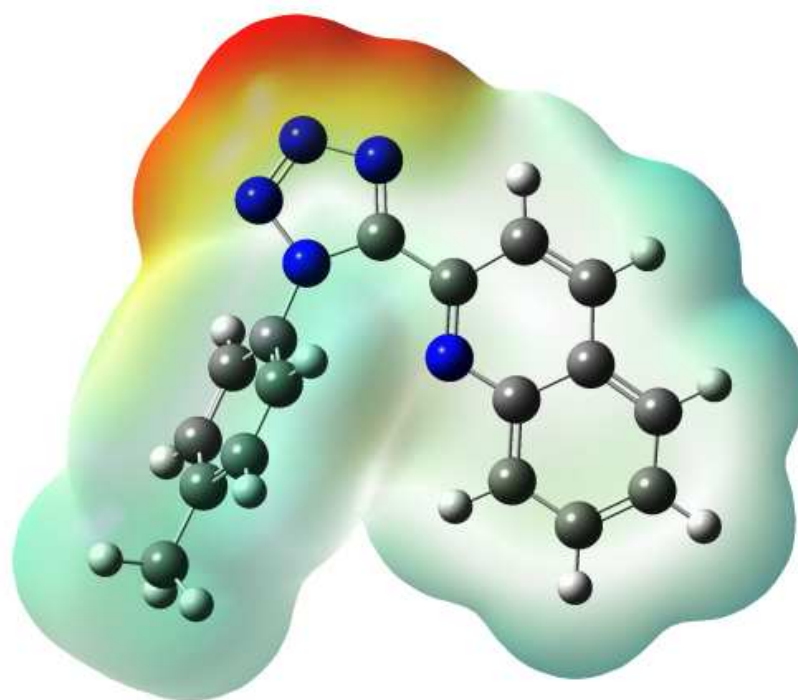


Fig. 7.

Highlights

- Tetrazoles are well-known bioactive compounds.
- Tetrazole-heterocycle hybrids exhibited excellent binding with enzymes.
- Quinoline-tetrazole hybrids are better bio-active compounds than other hybrids.
- The Molecular electrostatic potential results indicated the active regions.